SH25C-2098

LA-UR-20- 29579

A Three Dimensional Map of the Heliosphere from IBEX*

Daniel B. Reisenfeld[1], Maciej Bzowski[2], Herbert O. Funsten[1], Jacob Heerikhuisen[3], Paul H. Janzen[4], M.A. Kubiak[2], David J. McComas[5], Nathan A. Schwadron[6], Justyna Sokol[5], and Eric J. Zirnstein[5]

Abstract

The *Interstellar Boundary Explorer* (*IBEX*) mission has shown that variations in the ENA flux from the outer heliosphere are associated with the solar cycle and longer-term variations in the SW. In particular, there is a good correlation between the dynamic pressure of the outbound SW and variations in the later-observed *IBEX* ENA flux. The time difference between observations of the outbound SW and the heliospheric ENAs with which they correlate ranges from approximately two to six years or more, depending on ENA energy and look direction. This time difference can be used as a means of "sounding" the heliosheath, that is, finding the average distance to the ENA source region in a particular direction. We apply this method to build a three-dimensional map of the heliosphere. We use *IBEX* ENA data collected over a complete solar cycle, from 2009 through 2019, corrected for survival probability to the inner heliosphere. We divide the data into 56 "macro-pixels" covering the entire sky, and as each point in the sky is sampled once every six months, this gives us a time series of 22 points per macro-pixel on which to time-correlate. Consistent with prior studies and heliospheric models, we find that the shortest distance to the heliopause d_{HP} is slightly south of the nose direction (d_{HP} ~ 110 – 120 au), with a flaring toward the flanks and poles (d_{HP} ~ 160 – 180 au). The heliosphere extends at least ~350 au tailward, which is the distance limit of the technique.

[1] Los Alamos National Laboratory, Los Alamos, NM, USA
[2] Space Research Centre of the Polish Academy of Sciences, Warsaw, Poland
[3] The University of Waikato, Hamilton, New Zealand
[4] The University of Montana, Missoula, MT, USA
[5] Princeton University, Dept. of Astrophysical Sciences and Princeton Plasma Physics Laboratory, Princeton, NJ, USA
[6] University of New Hampshire, Durham, NH, USA
[7] Southwest Research Institute, San Antonio, TX, USA

* Reisenfeld et al., *ApJS*, 254, 40, 2021

Separating Ribbon from Globally Distributed Flux (GDF)

It is first necessary to remove the IBEX Ribbon from the sky maps to which we are applying the sounding method, as the GDF ENAs are formed in the inner heliosheath, which is the region responding most immediately to the SW dynamic pressure changes, whereas the Ribbon is likely formed in the outer heliosheath. Because of the low statistics per pixel, previous Ribbon separation methods (e.g. Schwadron et al. 2018, Dayeh et al. 2019) use maps averaged over multiple years to improve statistics. However, to apply the sounding method, we need the best time resolution available, which requires carrying out Ribbon separation in 6-month sky maps. We apply a new technique where we average the flux over a 24° longitude range (in a ribbon-centered frame) before carrying out the separation. As an example, below we show the separation technique applied to the 5 IBEX-Hi energy steps for skymaps collected in the second half of 2013.

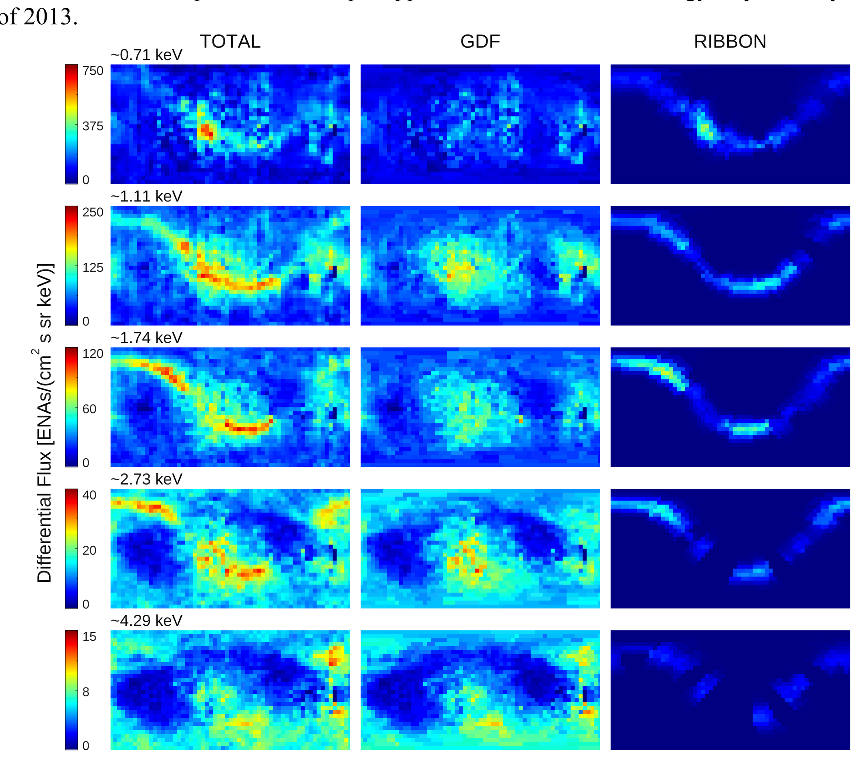

Calculating the Round Trip Time

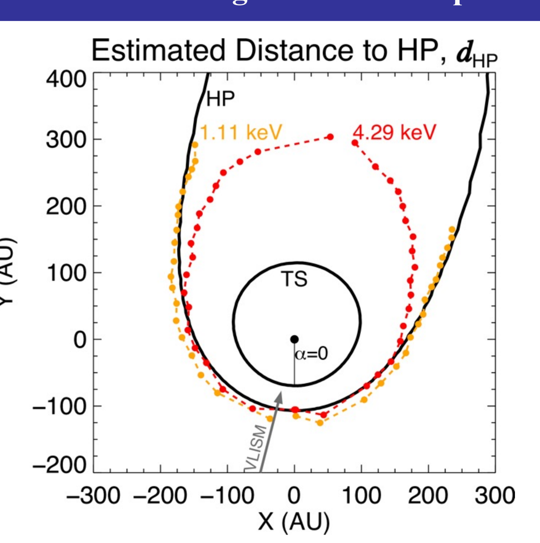

From Zirnstein et al. 2018, *Ap. J.*, 859, 104.

Zirnstein et al. (2018) used a heliosphere simulation to test the idea that one can accurately sound the distance to the heliopause by correlating the observed solar wind dynamic pressure at 1 AU with the ENA flux observed years later. A pressure disturbance is "propagated" through their model, and a simulated ENA flux is calculated. Employing the method described below, the colored curves in the figure show the estimated location of the heliopause based on observations of 1.11 keV ENAs (orange) and 4.29 keV ENAs (red). We see that in the noseward hemisphere, the HP position is accurately determined for both energies. The boundary based on the 4.29 keV ENA is underestimated in the tail direction because of the loss of heliosheath protons to charge exchange before they can propagate to the HP. Here, we nevertheless apply the sounding method to the whole sky, understanding that in the downwind direction, any resulting heliopause distances serve as lower limits. The true heliopause distance could be much further downstream.

The "traceback time" method: Given a solar wind disturbance propagating outward at the solar wind speed v_{SW} in a particular latitude λ and longitude b (as determined by IPS analysis), the time it takes for the effect of that disturbance to be observed in the return ENA signal is estimated by:

$$t_{ENA}(\lambda, b) = \frac{D_{TS}}{v_{SW}(\lambda, b)} + \frac{3}{2}\frac{T_{IHS}}{v_{ms}} + \frac{1}{2}\frac{T_{IHS}}{v_{ENA}} + \frac{D_{TS}}{v_{ENA}}$$

Where D_{TS} and T_{IHS} are the (unknown) termination shock distance and inner heliosheath thickness, v_{ms} is the magnetosonic speed (the speed at which a pressure disturbance propagates through the sub-sonic heliosheath, taken to be 300 km/s), and v_{ENA} is the speed at which ENAs of a given energy propagate back to IBEX. The first term on the right is the time it takes the solar wind to propagate to the TS. Only after the pressure wave propagates to the heliopause and reflects can the plasma pressure in the IHS readjust to its new, higher, level. Thus, the second term on the right approximately accounts for the time it takes the pressure wave to travel to the heliopause and reflect halfway back towards the TS, i.e., 3/2 T_{IHS}. The third term accounts for the time it takes ENAs to travel from halfway through the IHS to the TS. The fourth term accounts for the time it takes ENAs to travel from the TS to IBEX.

Note that this method assumes a static heliosphere; that is, the TS and HP distances are not changing in time. Time-dependent heliosphere models that simulate the solar cycle indicate that these boundaries do change. Typically, the models show a change in the upwind direction for D_{TS} of ±10 AU and a change in D_{HP} of ±5 AU (see Izmodenov et al. 2008, 2005). This is of small concern for this study because this is at the level of the resolution of the traceback method.

Sounding the Distance to the Heliopause: Correlating ENA-Derived Pressure with 1 AU SW Dynamic Pressure

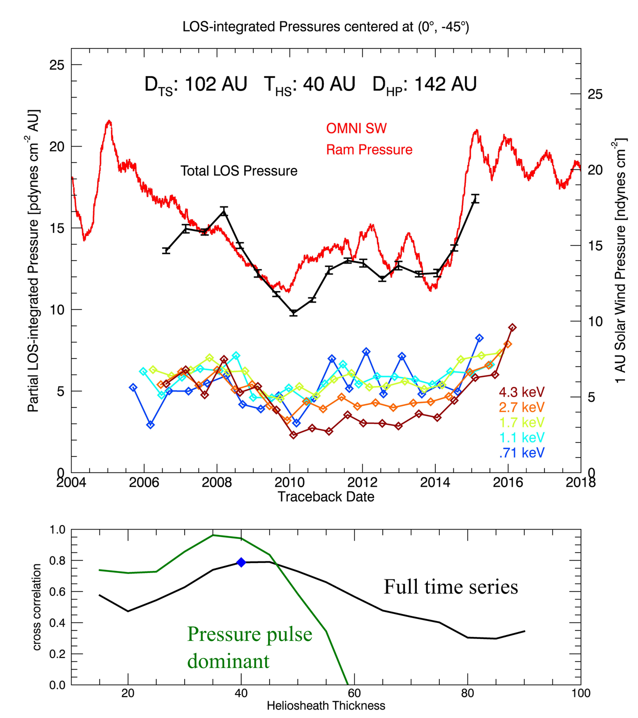

To the left are shown partial- and total line-of-sight (LOS)-integrated plasma pressures in the inner heliosheath versus traceback time. The partial LOS-integrated pressures are derived from the ENA flux using the following equation:

$$\Delta(P_S \cdot L)_i \cong \frac{4\pi\sqrt{2m}}{3n_H}\int_{E_i}^{E_{i+1}} \frac{\sqrt{E}}{\sigma(E)} j_{\text{ENA}}(E_i)\left(\frac{E}{E_i}\right)^{-\gamma_i} dE$$

where j_{ENA} is the ENA flux for energy step i, γ is the spectral index for the flux between E_i and E_{i+1}, m is the proton mass, n_H is the interstellar neutral hydrogen density, and $\sigma(E)$ is the charge-exchange cross section.

In this example, the ENA data are taken from a "macro-pixel" centered at the ecliptic coordinate (0° lat, -45° long). The total LOS-integrated pressure (black curve, unscaled) in this direction is calculated from the partial pressures for the time range when the traceback times for all five ESAs overlap. Also shown is the 1 AU SW dynamic (ram) pressure calculated from the OMNI-2 dataset (red line) plotted for the actual time of observation (6-month smoothing applied).

The "best" traceback time is prescribed by evaluating the correlation between the total LOS-integrated plasma pressure and the 1 AU SW dynamic pressure (lower panel). We carry out two correlations, one for the full time series (black curve) and one for the second half of the time series only (green curve), where the pressure jump in 2014 dominates. Using these as guides, the heliosheath thickness value that optimizes both of these simultaneously (which may not be the best correlation for either) is determined to arrive at the best choice for HS thickness.

The Dimensions of the Heliosphere as Derived from Pressure Correlation

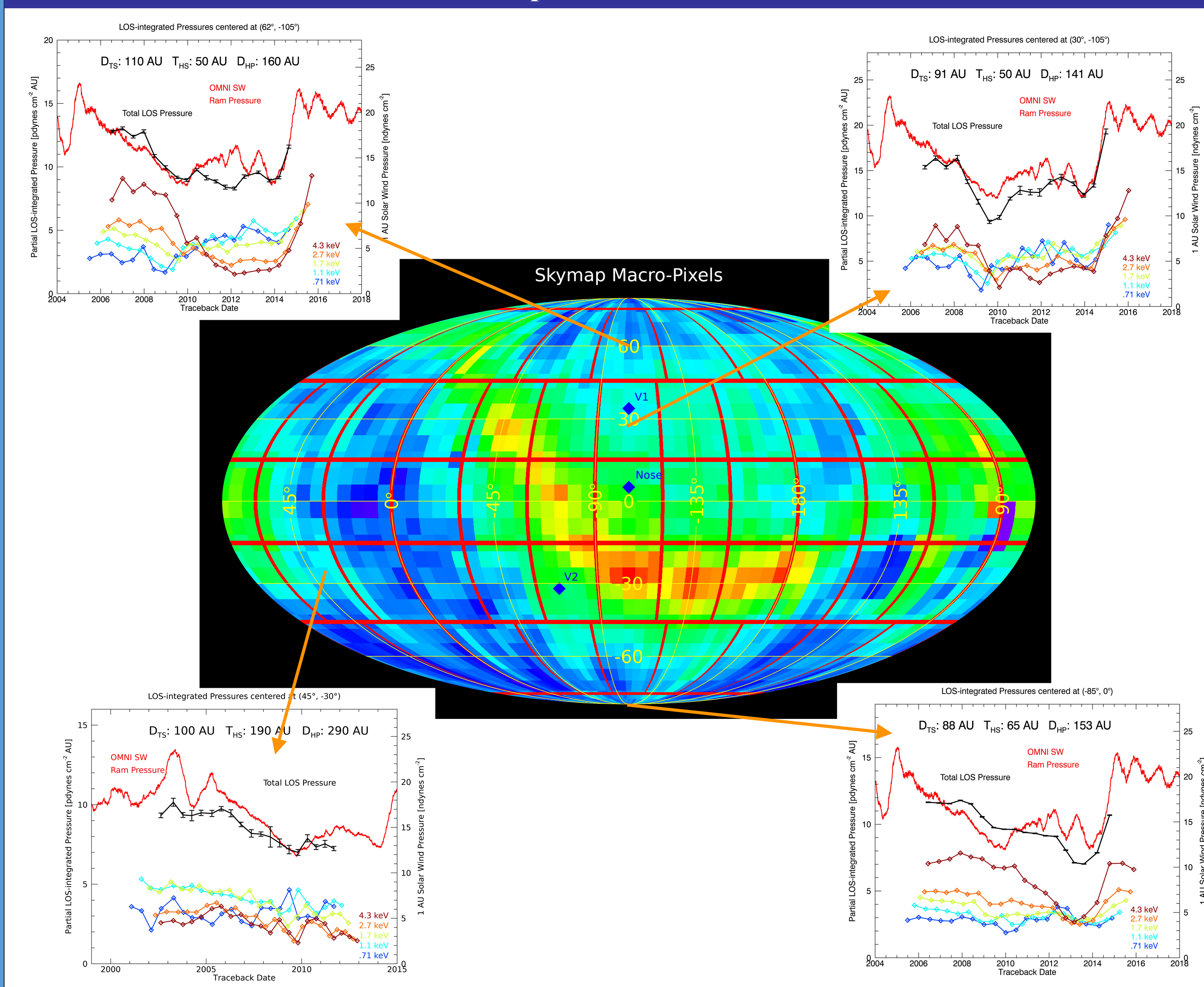

We have divided the full sky into 56 regions. We select macro-pixels large enough for reasonable statistical variation, but small enough to be sampling a region of common spatial evolution. For each region we apply the pressure correlation method to come up with a best-fit traceback time, and from that an estimate of the dimensions of the heliosphere in that direction. Above, we overlay the boundaries of the 56 macro-pixels on a representative skymap.

Modeling of the Termination Shock

The pressure correlation method does not uniquely determine both the TS distance and the heliopause distance. Since the TS distance is perhaps better constrained by other methods, we use various models for the shape of the TS and then evaluate the distance to the heliopause using these TS distances. We have tried three models:

1. A uniform 100 AU radius TS model. This is chosen to demonstrate that the HP distance variation is not driven by the choice of TS model.
2. A TS shape derived from the MHD model of Zirnstein and Heerikhuisen (the Z-H model). This model, although time-independent includes fast wind above |35°| latitude, and slow wind below. It also assumes a constant SW dynamic pressure as a function of latitude, so it turns out that the shape of the TS is insensitive to the choice of the slow/fast wind boundary, the TS location is determined by the SW pressure, not the SW speed.
3. The spherical TS shape determined by an analysis of anomalous cosmic rays (ACRs) measured by the Voyager spacecraft as they traversed the HS. The TS is taken to be spherical with a radius of 117 au, but not centered on the Sun. This model was recently published in McComas et al. 2019.

Termination shock derived from Voyager ACR observations

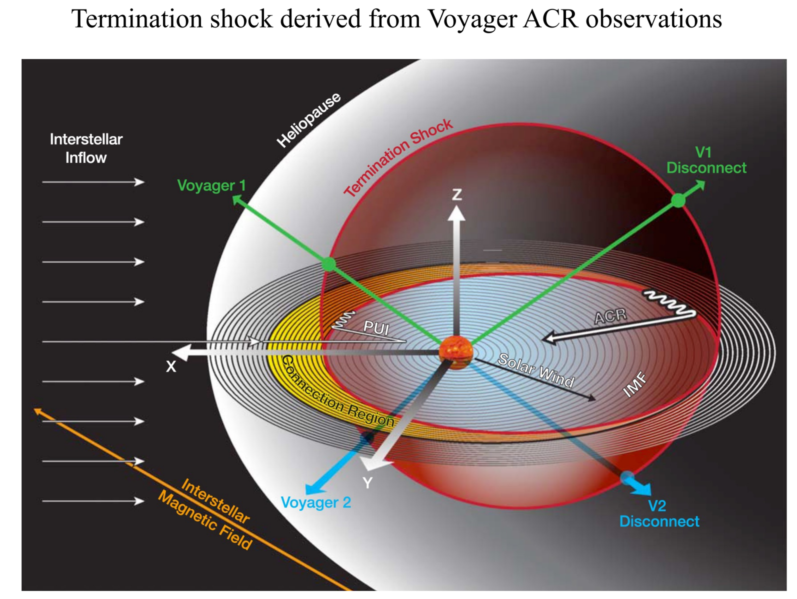

From McComas et al. 2019, *Ap. J.*, 884, 145.

The 3D Heliosphere

Using the three different TS models, we determine the distances to the HP for the 56 macro-pixels using the IBEX separated GDF maps. Below are projections of a 3-D rendering of the resulting HP shape for the case of the Zirnstein-Heerkihuisen TS model. The TS model is rendered in the interior of the HP, so that a sense of the thickness of the heliosheath is portrayed. All three models give similar qualitative results, although there are differences when examined in detail (see Voyager comparison below).

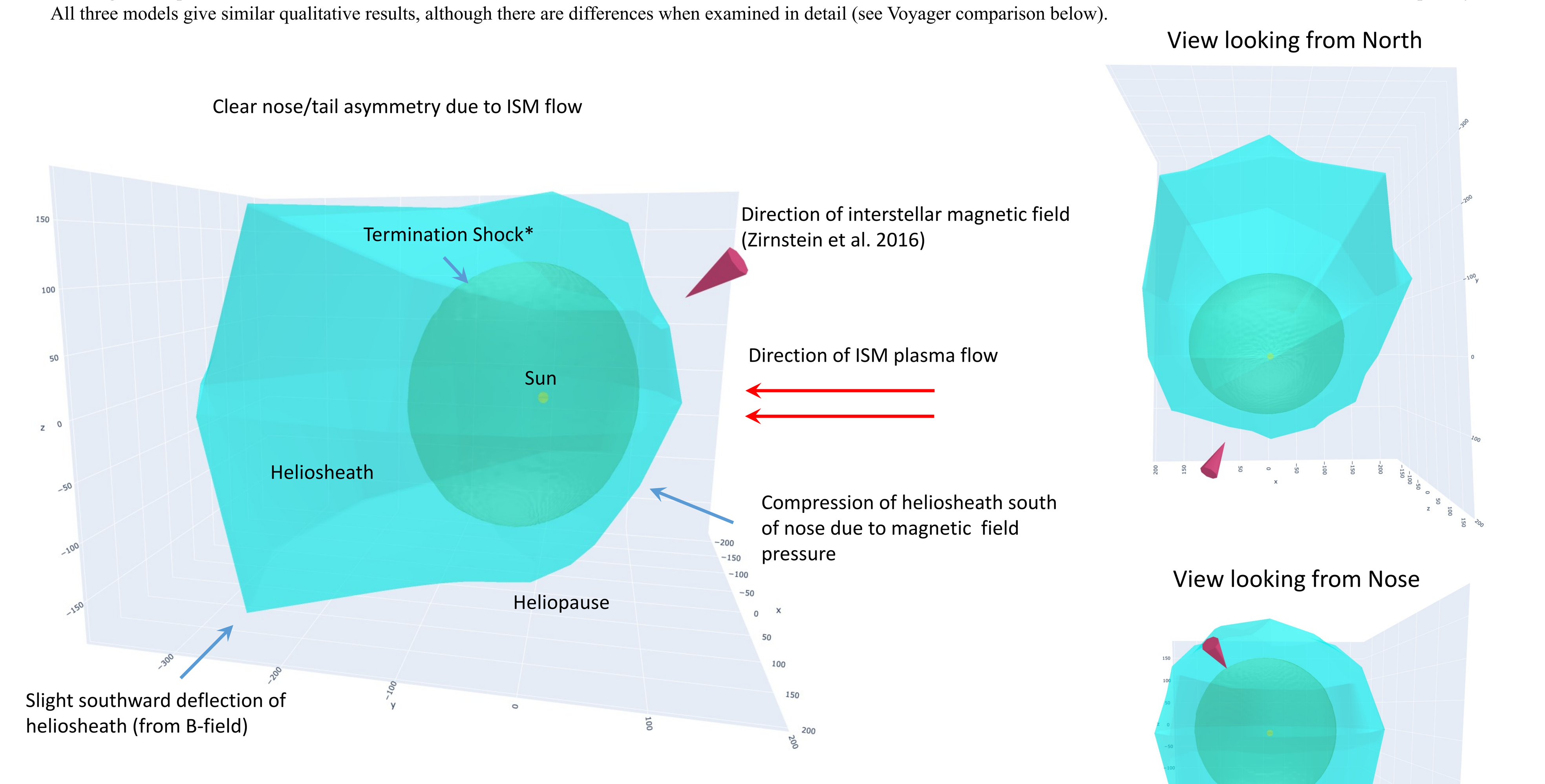

*Zirnstein-Heerkhuisen TS model

Comparison to Heliosphere Models

How does the IBEX-based empirically determined heliosphere shape compare to theoretical models? Below we give a comparison. We again point out that in the downwind direction the extent of the HP should be taken as a lower limit. The true distance to the HP could be much farther. That said, the ~200 au extent of the heliotail suggested by the "round heliosphere" model of Dialynas et al. is not consistent with our observations. Furthermore, our observations do not support the large poleward extent of the HP suggested by the Opher et al. "croissant" model. Thus, the Pogorelov et al. model is the most consistent with the IBEX observations.

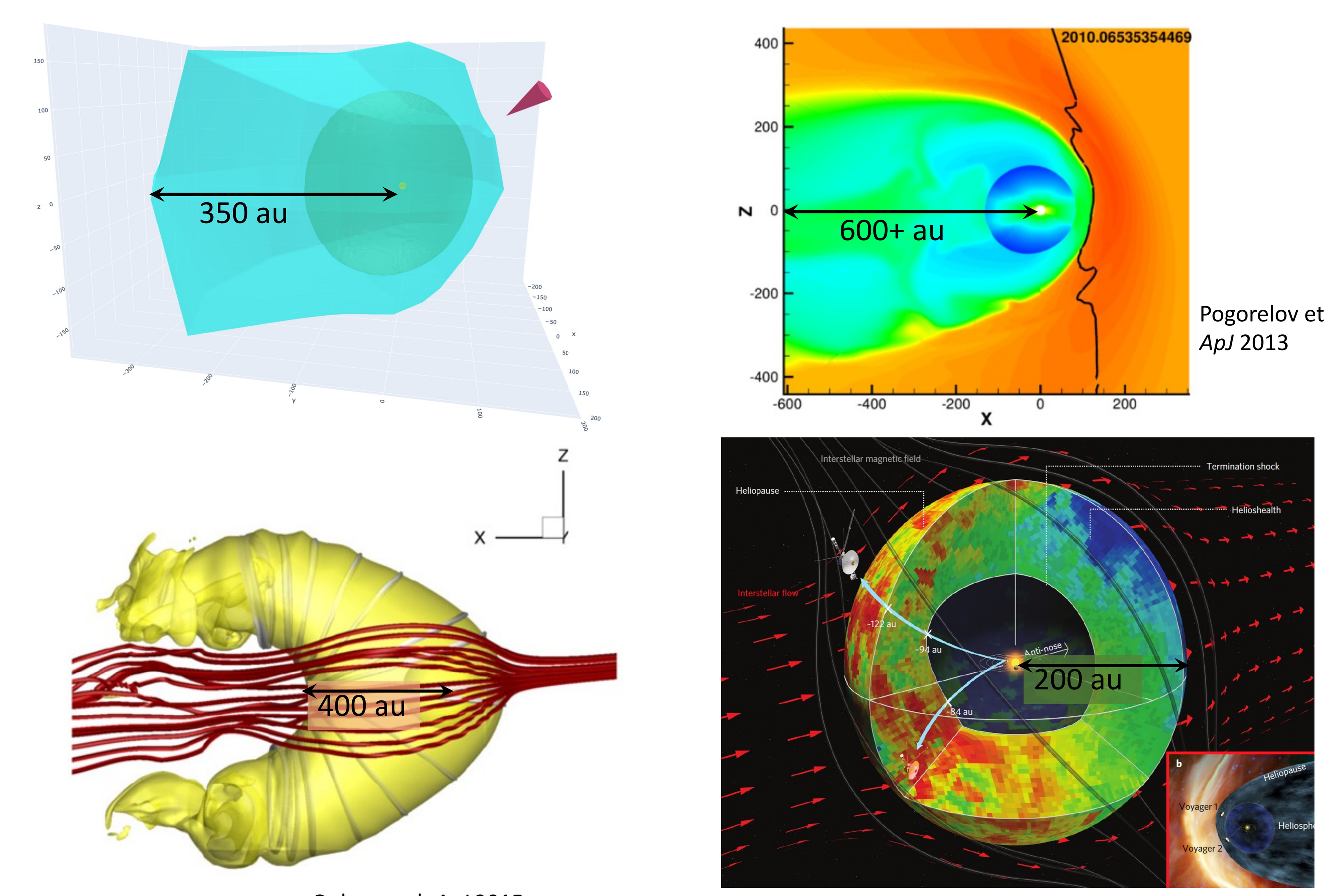

Pogorelov et al. *ApJ* 2013

Opher et al. *ApJ* 2015

Dialynas et al. *Nature Astron.* 2017

Comparison to Voyager Crossings and Conclusions

Comparison of heliosheath boundary distances along the Voyager radials to the Voyager crossing distances. For all models the HP distances are in agreement with the Voyager crossing distance, to within the estimated 10 au uncertainty of the sounding method in these directions. Heliosheath thicknesses are also in reasonable agreement with the observed thicknesses, with the exception of the 100 au TS model at V2.

	Model	Term Shock Distance	Heliosheath Thickness	Heliosheath Thickness Δ from Voyager	Heliopause Distance	HP Distance Δ from Voyager
Voyager 1	*Actual*	*94*	*28*	--	*122*	--
	100 au TS	100	35	7	135	13
	Z-H model	91	40	12	131	9
	Voy TS model	91	40	12	131	9
Voyager 2	*Actual*	*84*	*35*	--	*119*	--
	100 au TS	100	10	-25	110	-9
	Z-H model	95	20	-15	115	-4
	Voy TS model	82	30	-5	112	-7

Conclusions

- With nearly a full solar cycle of IBEX observations, we have shown that the sounding method can be effectively used to determine the shape of the heliosphere.
- Regardless of the TS model, the shape of the heliopause is consistent: It is compressed southward of the nose, shows a distinct tail, and is deflected slightly southward in the downwind direction. This is consistent with expectations for the shaping of the heliosphere by the combined influence of the ISM direction and the LISMF direction.
- When comparing to theoretical heliosphere models, the IBEX-derived shape is most consistent with the "comet"-like description of Pogorelov et al. (2013).
- In the Voyager 1 direction, the derived heliosheath thickness is somewhat thicker than the thicknesses of 28 AU observed by V1, but only by ~10 au, which is within the uncertainty limits of the sounding method. The same is true for the distance to the HP.
- In the Voyager 2 direction, the derived heliosheath thicknesses are within uncertainty, except in the case of the constant 100 au TS model, but this is not surprising considering the arbitrariness of that model. In all cases the distances to the HP are in quite good agreement with the observed V2 HP crossing distance.